IJCRT.ORG ISSN : 2320-2882

INTERNATIONAL JOURNAL OF CREATIVE RESEARCH THOUGHTS (IJCRT)

An International Open Access, Peer-reviewed, Refereed Journal

FLC based MPPT Controller for Grid connected Photovoltaic systems for Power Quality Assessment

CA. BHASKAR
M.Tech Student
Department of EEE,
SKUCET, Ananthapuramu, India

Dr. P. SHASHAVALI
Assistant Professor (C)
Department of EEE,
SKUCET, Ananthapuramu, India

Abstract: **Islanding occurs when distributed generators (DGs) only supply electricity to local loads after the disconnected power grid. It has been stated that several islanding detection methods (IDMs) classified as remote, active, and passive can detect this undesirable state. The DG's controller is perturbed in functional approaches, causing a local yardstick to drift outside the acceptable range. Even in well-balanced islands, this disruption improves detection accuracy, but under normal operating conditions, it increases the total harmonic distortion of the output current (THDI). The impact of the modified sliding mode controller on power quality as a novel active IDM for grid-connected photovoltaic systems (GCPVS) with string inverters is investigated in this work. The positive voltage feedback (VPF) approach, a well-known active IDM, compare its performance. This evaluation is carried out for a 1 kW power GCPVS using the MATLAB/Simulink platform by evaluating the output current harmonics, THD, and efficiency under various penetration and disturbance levels. Because it changes the amplitude of the output current, the output data show that the proposed disturbance does not produce harmonics or subharmonics. As a result, it has little effect on power quality. The sliding mode-based IDM's performance is ultimately found to be reliable in terms of islanding detection and power quality**

Index Terms **- Communication Islanding Detection Method (IDM), power quality, sliding mode controller, Total Harmonic Distortion (THD), Voltage Positive Feedback (VPF).**

I. INTRODUCTION

Renewable energy solutions are increasingly being used in dispersed networks. In this regard, over 80 GW power of grid-connected photovoltaic systems (GCPVSs) were deployed globally in 2017, representing a 30% increase over the previous year [1]. Although these inverter-based resources provide clean, noise-free energy to the network, the power quality of the available energy suffers due to the addition of current harmonics. These harmonics can have an impact on the electrical network, resulting in unbalanced line voltages, voltage level variations, and line impedances. Given the widespread use of GCPVSs in distribution networks, one of the significant sources of harmonics is the inverter's current control loop, which is in charge of converting DC to AC power. Even though this power quality degradation is minimal in comparison to the novel switching patterns [2]- [4], active islanding detection techniques (IDMs) are now recognized as a new source of current harmonics [5].

A scenario known as islanding occurs when a portion of the utility, including a distributed generator (DG), is cut off from the network while continuing to supply power only to local loads. To ensure the security of the repair team and avoid the failure of delicate equipment, this status must be accurately defined [5]. In this context, the number of IDMs divided into local and remote groups has been reported [6]–[25].Remote communication is used between the DGs and the upstream substation. Islanding can be classified as occurring under non-signal-receiving conditions because the broadcast signal continuously monitors the connections of DGs to the electrical network [6–8].

The measurement of local parameters at the point of common coupling (PCC), as shown in Fig. 1, forms the basis for passive and active regional approaches. When islanding occurs, the active and reactive electricity sent to or received from the public grid is cut off. As a result, the voltage and frequency of the PCC experience abrupt fluctuations. Active techniques are recommended [16–25] to reduce the none-detection zone (NDZ) or states where IDM fails to detect islanding. Passive systems [9–

15] or a clearly defined local yardstick can be used to identify these deviations. The DG controller is continuously subjected to an intentional disruption in these methods to accelerate the divergence of PCC parameters during islanding events.

Active schemes include Active Frequency Drift (AFD) [16, 17], impedance measurement (IM) [18-20], voltage positive feedback (VPF) [21-24], and modified sliding mode controller (MSMC) [25]. Although the applied disturbance effectively reduces the NDZ, it also reduces the power quality of the output current. Harmonic distortion, as measured by total harmonic distortion, is the most concerning of all power quality concerns (THD). The injected disturbance should be limited to an upper limit to meet power quality standards. Tables I and II of IEEE Standard 1547-2008 [26] and IEC Standard 61727-2002 [27] list the permitted ranges of the local electrical amounts. In Table II, the even harmonics must be less than 25% of the odd harmonics.

The power quality analysis of the DG output power belonging to the used active IDMs was completed in [16]-[25], [28], and [29]. To meet the standards for a sample GCPVS, the ratio of the injected reactive power disturbance (Q) to the active power output (PDG) in AFD must be kept within the range of [-0.95%, 4.11%], according to literature [16]. The designed a traditional AFD technique to reduce the current THD (THDI) of a 300 W power PV system delivering a local load[17]. It has been discovered that, when compared to simple AFD, the same NDZ can be obtained with a 30% reduction in THDI. A high-frequency signal injection was presented in [18] using a high-frequency IM to categorize the islanded functioning mode. In multi-DG configurations, they recommend only using one inverter disturbance injection to maintain acceptable power quality. Otherwise, THDI may not be appropriate in some multiple DG situations. Investigated power quality evaluation using ten string inverters connected to the Brazilian electrical system [28]. The power analyser measured power factor, voltage THD (THDV), and THDI with a few loadings. The analysis of estimated data shows that the output energy meets the quality standards across a wide range of operating conditions, particularly at high penetration levels. At low-power generations, however, high THDI, THDV, and a low power factor have been observed [28]. [29] evaluated the effect of IM and AFD techniques on the power quality of a single-phase 1.5 kW power PV system. Even if THDI rises from 0.7% to 13% in the presence of IM disturbance, the average remains acceptable (3.7%). Further more, THDI increases when the GCPVS produces low power. This occurs because the fundamental harmonic of the reference curve is reduced while the disturbance size remains constant.

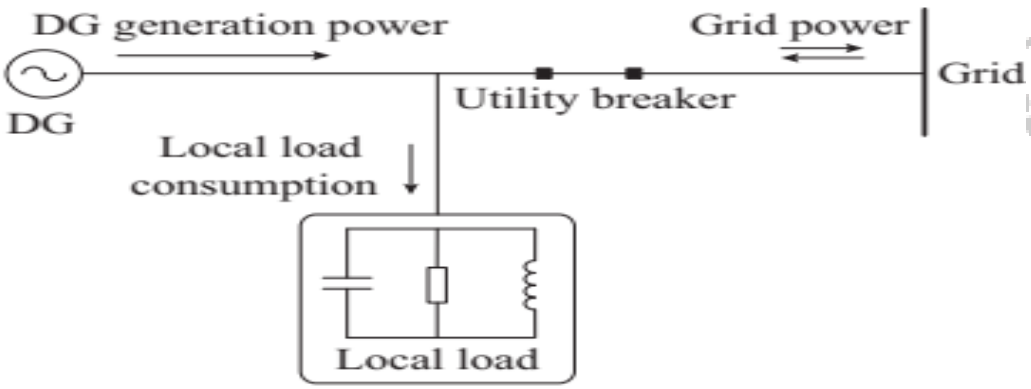

Fig. 1. Interconnection of DG and local load to electric network.

Power quality must be met in states where GCPVS output power is less than 41.3% of its nominal value. Simulations of AFD with positive feedback (AFDPF) have been built. THDI exceeds the standard limit when the output power falls below 400 W (26.66% of nominal power) [29]. According to the study, the amount of GCPVS output power influences how quickly THDI rises. Because of the interference injected into the frequency or angle of the output current, the current control loop is also known as the main harmonic generator.

TABLE I
SUMMARY OF STANDARDS CORRESPONDING TO INTERCONNECTION OF GCPVS TO GRID

Standard	Nominal power (kW)	Maximum THD_I (%)	Voltage range (%)	Frequency range (Hz)
IEEE Standard 1547-2008	10	5	88-110	59.3-60.5
IEC Standard 61727-2002	30	5	88-110	49.0-51.0

This paper investigates the impact of a modified sliding mode controller as a new VPF-based active IDM on GCPVS output power quality. Because the disturbance enters the inverter's voltage control loop, the proposed method will only change the amplitude of the output current rather than the frequency or angle. As a result, its impact on the power quality of the distribution network is hardly comparable to that of a conventional VPF.

II. DESCRIPTION OF MODIFIED SLIDING MODE CONTROLLER

Following an islanding event, VPF becomes an active IDM to destabilize PCC voltage. This is accomplished by tuning the inverter's active power output by injecting a VPF into the d-axis reference current. When the PCC voltage rises after islanding, the reference current, active power output, and PCC voltage all rise. This voltage's magnitude gradually increases until it exceeds the over-voltage relay setting (1.1 p.u.). In the event of a PCC voltage drop, the output power and voltage are reduced until the under-voltage (UV) relay setting (0.88 p.u.) is reached [21]-[24].The sliding mode controller uses the VPF concept to represent a new active IDM [30]. In Fig. 2(a), the maximum power point (MPP) current (IMPP) in terms of the maximum power point (MPP) voltage (VMPP) can be calculated using the following linear equation:

$$S(I_{PV}, V_{PV}) = I_{PV} - bV_{PV} + ref \qquad \ldots.(1)$$

Where b should be determined using pairings of V_{MPP} and I_{MPP} at different irradiance levels in conjunction with the least square error approach, and ref is a variable parameter that calculates MPP in every climate scenario. This factor should be specified in the inverter's voltage control loop utilizing classic MPP tracking (MPPT) approaches such as perturb and observe (P&O). The sliding surface parameter $S(I_{PV},V_{PV})$ value of the sliding mode controller governs the boost converter's operational state. When $S(I_{PV}, V_{PV}) > 0$, the control switch opens, and the inductor discharges. This reduces the PV array's current while increasing its voltage. If the converter switch closes in the $S(I_{PV}, V_{PV})$ 0 state, the inductor will be charged, the PV current will increase, and the voltage will fall. As a result, the operating point would be regulated so that the GCPVS operates around $S(I_{PV}, V_{PV}) = 0$, or MPP [30]. The sliding mode controller schematic diagram for GCPVS with string inverter is illustrated in Fig. 2(b)

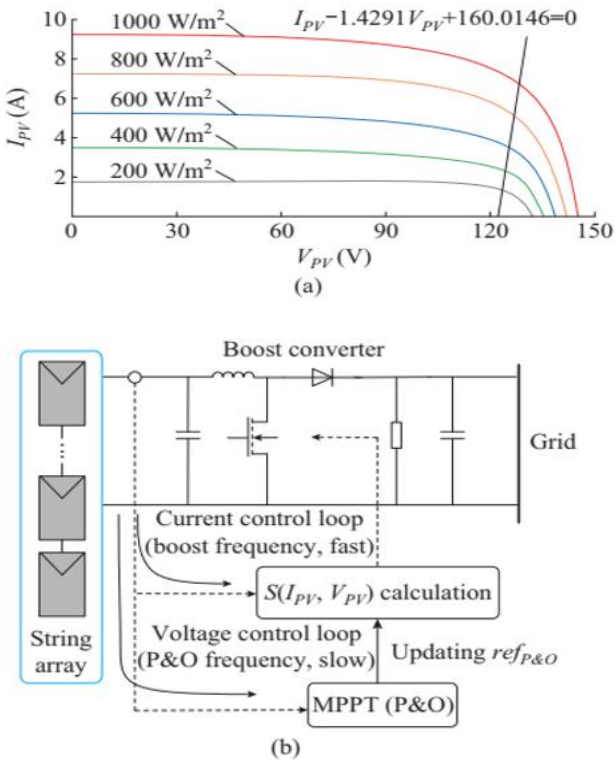

Fig. 2. Sliding mode MPPT technique. (a) Characteristics locus of V_{PV} and I_{PV} . (b) Schematic diagram.

III. ISLANDING DETECTION OF MODIFIED SLIDING-MODE CONTROLLER

This section describes the case study system and offers a few islanding scenario-based reasons for the upgraded sliding-mode controller. The disturbance gain selection criteria are also explored in depth. The proposed method application to a sample system is shown schematically in Fig. 3. The PV array, which consists of four 250 W QPRO-G2 modules, is linked to the single phase 1 kW power inverter. The specifications for this module are listed in Table III under standard test circumstances (STC), which are 1000 W/m2 of radiation and 25 °C for the cell temperature.

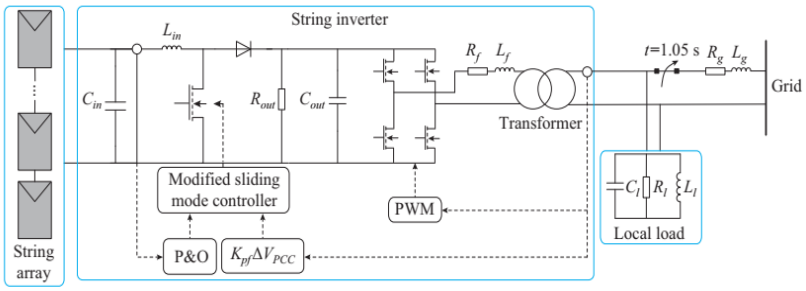

Fig. 3. Schematic of case study system.

To meet the islanding standard requirements, the local load is modelled as an RLC circuit with a 2.5 quality factor Qf and a resonance frequency of roughly 50 Hz. Ultimately, this load and GCPVS are connected to PCC's single-phase 230 V, 50 Hz network. The improved sliding mode controller should lower active power output and, as a result, PCC voltage to the minimum acceptable level for islanding classification (0.88 p.u.). The islanding in the case study system was simulated by turning on the circuit breaker next to the PCC in Fig. 3 at t = 1.05 s. As previously stated, the local load has been configured to absorb all generated power at STC with Qf = 2. 5 as a worst-case scenario in compliance with IEEE Standard 929-2000 [31].

Table II
DATA OF QPRO-G2 250

Parameter	Value
Maximum power (P_{MPP})	250 W
Short-circuit current (I_{SC})	8.94 A
Open-circuit voltage (V_{OC})	37.78 V
Maximum power point current (I_{MPP})	8.45 A
Maximum power point voltage (V_{MPP})	29.89 V
Temperature coefficient of I_{SC}	3.57 mA·°C^{-1}
Temperature coefficient of V_{OC}	−124.67 mV·°C^{-1}
Temperature coefficient of P_{MPP}	−1.075 W·°C^{-1}

IV. POWER QUALITY ASSESSMENT

The effectiveness and performance of the sliding-mode-based IDM are evaluated using the current harmonics THDI. According to scientific sources, the power quality criteria do not include efficiency. However, because the proposed IDM differs from the MPP in terms of the GCPVS operating point, the variation in efficiency is also assessed. In an electrical system, harmonics cause voltage or current to vary from their original sinusoidal waveforms. This deviation can be measured using THD, the ratio of the root-mean-square (RMS) voltage or current of the harmonics to the fundamental component. According to IEEE Standard 1547-2008 and IEC Standard 61727-2002, THDI should be limited to 5%. Moreover, harmonic component values should be restricted to those in Table II.

Table III
DISTORTION LIMITS

Odd harmonic number (*h*)	Distortion limit (%)
3-9	4.0
11-15	2.0
17-21	1.5
23-33	0.6
>33	0.3

V. FUZZY and ANN CONTROLLER

Artificial controlling method has been widely applied in solar MPPT application now a days, and fuzzy logic control is the most popular method among them. The trend of this method is mainly due to the invention of micro controller, in which complicated coding and algorithm can be easily programmed and implemented. Low cost micro controllers, such as Atmega8 and digital signal processor or FPGA have been proven functional in the concept of fuzzy logic control. Fuzzy logic control is mainly comprised of three stages, which are fuzzification, fuzzy rule base table and defuzzification. In the fuzzification stage, the main purpose is to transform the numerical variables into linguistic fuzzy set notation. By using membership function as Shown in Fig.4, the level or the range of each linguistic label can be determined. The accuracy of fuzzy logic is greatly influenced by the number of membership function, where with greater number of membership functions, the higher the controller accuracy will get. Normally, the range of membership functions is between 5 to 7. The example of five fuzzy level is depicted in Fig.4: NB (negative big), NS (negative small), ZE (zero), PS (positive small), and PB (positive big). The variables a, b are the values that are covered by each of the membership function. Some membership functions are made less symmetric to prioritize and optimize the particular fuzzy level. For example denser function in the middle in order to improve the sensitivity of PV voltage at the MPP. In solar MPPT system, the usual inputs of fuzzy controller are error, E and the change of error, ΔE.

However, for solar PV system, most will choose the slope of P-V curve, dP/dV as the error equation since zero value will be obtained at MPP. Equation (2) and (3) depict the error and the change of error. In some literatures, dP and dV were chosen as the inputs of the controller.

$$E(k) = [P(k) - P(k-1)]/[V(k) - V(k-1)] \quad \ldots (2)$$

$$\Delta E(k) = E(k) - E(k-1) \quad \ldots (3)$$

Table IV. Rule Base Table

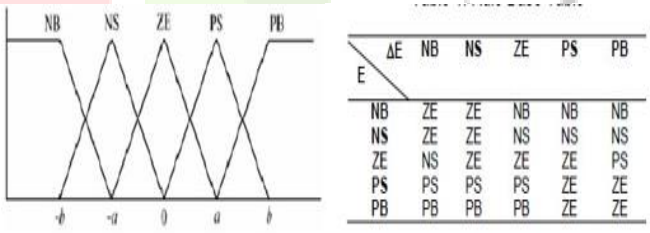

E \ ΔE	NB	NS	ZE	PS	PB
NB	ZE	ZE	NB	NB	NB
NS	ZE	ZE	NS	NS	NS
ZE	NS	ZE	ZE	ZE	PS
PS	PS	PS	PS	ZE	ZE
PB	PB	PB	PB	ZE	ZE

Fig. 4. Membership Function of FLC

Besides fuzzy logic control, neural network is another method that suits the operation of micro controller and digital signal processor, where the majority are software programming based devices. Both methods need great software familiarity and knowledge to ensure the system performs as desired. Usually, the basic structure of a single neural network consists of three different layers, which are input, hidden and output layer as presented in Fig.5.

The characteristics such as the number of input nodes and the number of hidden layers are defined by the designer. As described, the higher the number of hidden layer, the more precise the system will be. Normally, in solar MPPT, the input of the neural network can be in any kind of combination, such as surrounding condition (irradiance, temperature) or PV parameters (Voc, Isc), while the output can only be one, either duty cycle or reference voltage. Apart from the number of hidden layer as mentioned

previously, another important factor that contributes to the system accuracy is the training given. Since each of the PV array has different characteristics, thus, training has to be given so that the system can precisely represent the particular PV array.

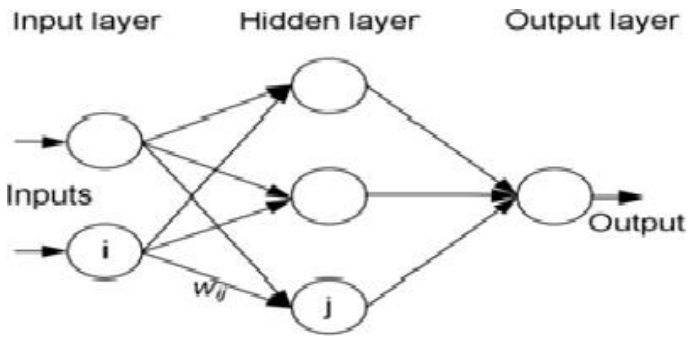

Fig. 5. Fundamental of Neural Network

Along the training process, the form of the input and output will be observed and recorded from time to time, in which the duration could be a few months or even a year. From the outcome of the training, the weight of each link for example, can be accurately identified. A multi-level neuro-fuzzy model for MPPT, which comprises of fuzzy logic controller and three multi-levels feed forward neural network. The system has been proven capable of yielding higher efficiency and representing complex and nonlinear behavior of PV array under wide range of operation circumstance, compared to conventional neural network algorithm. However, the main disadvantage of neural network is unavoidable, where the system needs to be periodically trained to ensure highest accuracy since the PV array's characteristic will vary with time.

VI. SIMULATION RESULTS AND DISCUSSIONS

The Fig.6 shows a schematic of the sample system with the suggested approach applied to it and Fig.7 is the corresponding block diagram for MPPT with modified sliding mode controller. The single phase 1kw power inverter has been linked to a PV array consisting of four 250 W QPRO-G2.

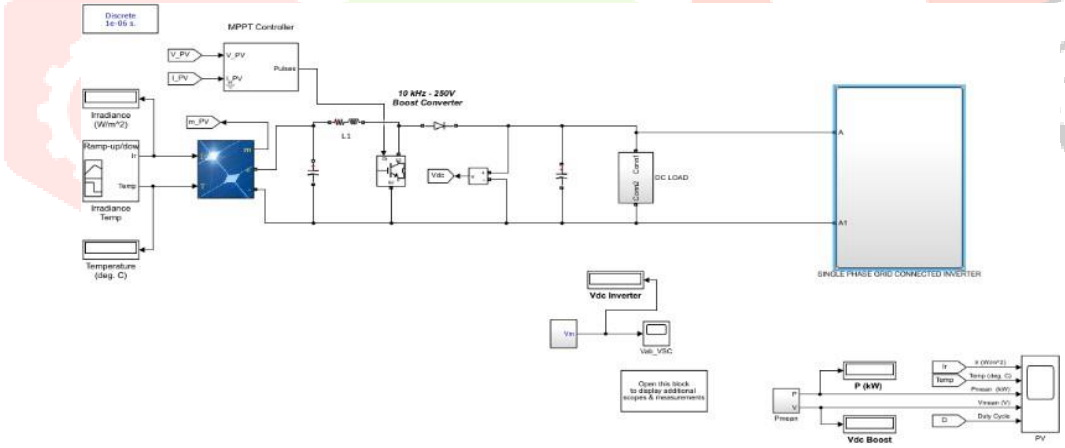

Fig.6. Schematic of case study under evaluation.

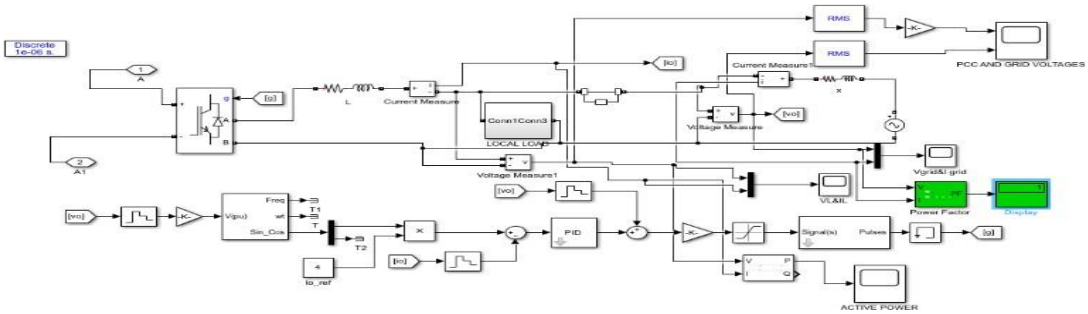

Fig. 7. Conventional MPPT with modified sliding mode controller

Fig.7 shows the grid connected inverter with Conventional MPPT. Here P&O algorithm and Sliding mode controller used for extracting the maximum power from the PV.

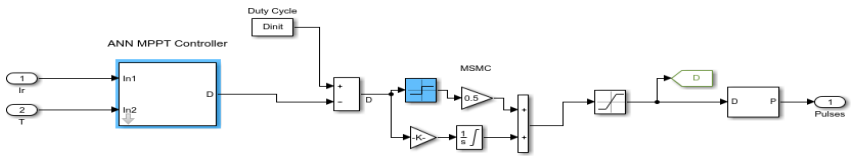

Fig.8. ANN MPPT

Fig.8 shows the structure of Artificial Neural Network based MPPT. Here ANN-MPPT used for extracting the maximum power from the PV.

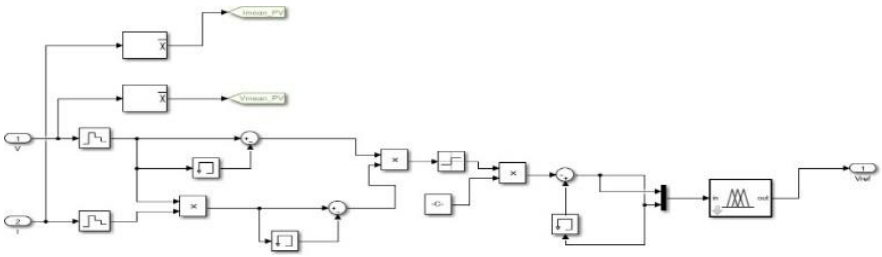

Fig.9. FLC MPPT

Fig.9 shows the structure of Fuzzy Logic Controller based MPPT. Here FLC-MPPT used for extracting the maximum power from the PV. To meet the minimal standard setting (0.88p.u.) for Islanding classification, the updated sliding mode controller, To meet the minimal standard setting (0.88p.u.) for Islanding classification, the updated sliding mode controller should reduce active power output and as a result, PCC voltage. For the case study system, Islanding was simulated by activating the circuit breaker beside PCC in Fig.7 at t=1.0s. As previously stated, the local load was programmed to consume all produced power at STC with quality factor=2.5 as a worst-case scenario and in accordance with IEEE Standard 929-2000 [31]. To fulfil the Islanding standard criteria, the local load is modelled as an RLC circuit with a resonance frequency of roughly 50 Hz and a 2.5 quality factor. At PCC, this load and GCPVS are eventually connected to the single- phase 230 V, 50 Hz network. Fig.7 shows the block diagram of conventional MPPT with FLC.

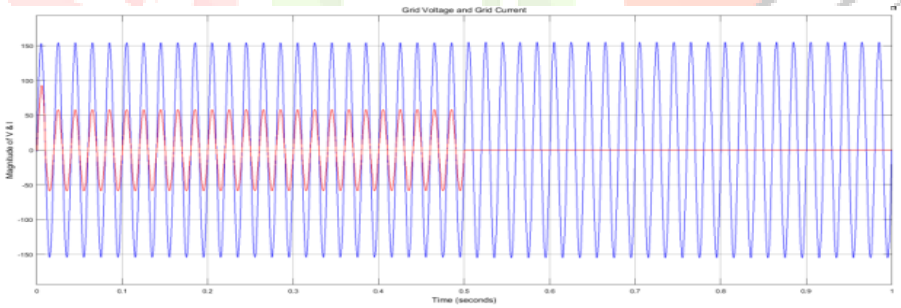

Fig.10. Grid voltage and Grid current for FLC

Grid voltage and grid current with FLC-MPPT are shown in Fig.10. from this figure, it is identified that grid voltage is constant over the simulation period of 1 second, grid current changing from maximum to minimum and this change occurred at 0.5 seconds.

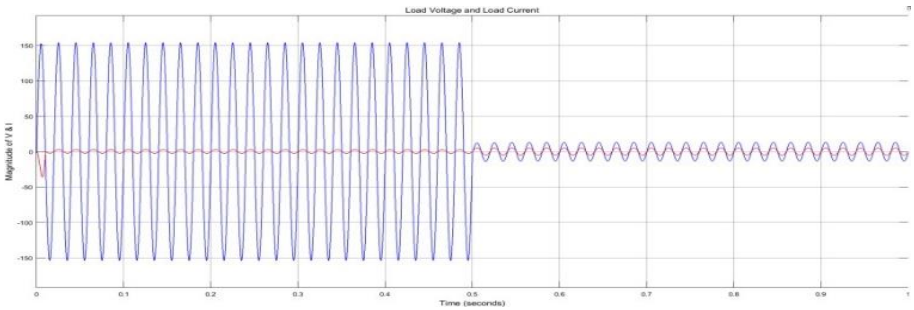

Fig.11. Load voltage and Load current for FLC

Load voltage and load current with FLC-MPPT are shown in Fig.11. from this figure, it is identified that load voltage is decreased from maximum to minimum at 0.5 seconds. Grid current changing from minimum to maximum and this change occurred at 0.5 seconds. Grid voltage and grid current with ANN-MPPT are shown in Fig.12. from this figure, it is identified that grid voltage is constant over the simulation period of 1 second, grid current changing from maximum to minimum and this change occurred at 0.5 seconds.

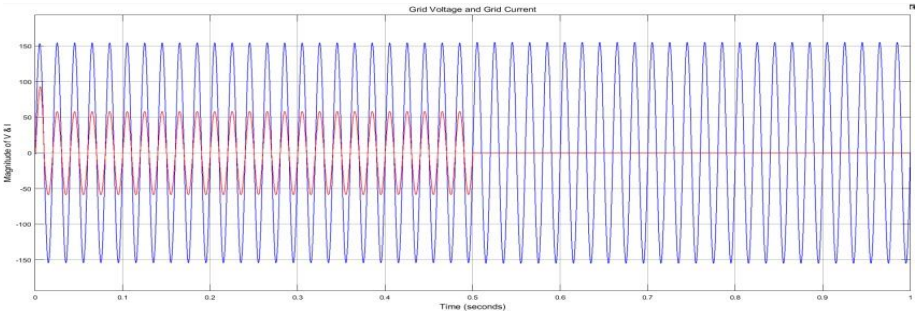

Fig.12. Grid voltage and Grid current for ANN

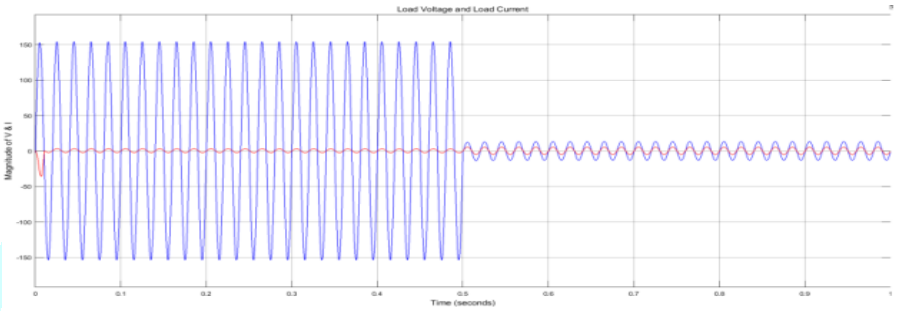

Fig.13. Load voltage and Load current for ANN

Load voltage and load current with ANN-MPPT are shown in Fig.13. from this figure, it is identified that load voltage is decreased from maximum to minimum at 0.5 seconds. Grid current changing from minimum to maximum and this change occurred at 0.5 seconds.

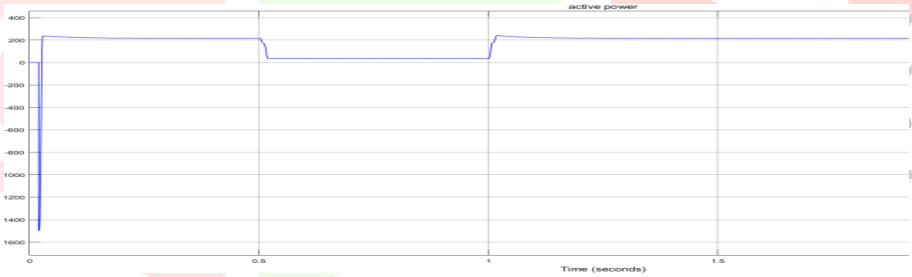

Fig.14. Active power for ANN MPPT

From Fig.14 illustrates the variation of active power with ANN-MPPT controller. Active power first falls to 1400 watts and recovered within short span. The active power is changing from 200 watts to 20 watts at 0.5 seconds and then 20 watts to 200 watts at 1 second. From Fig.15 illustrates the variation of active power with FLC-MPPT controller. The active power is changing from 200 watts to 20 watts at 0.5 seconds and then 20 watts to 200 watts at 1 second. The peak overshoots are reduced as compared with ANN-MPPT.

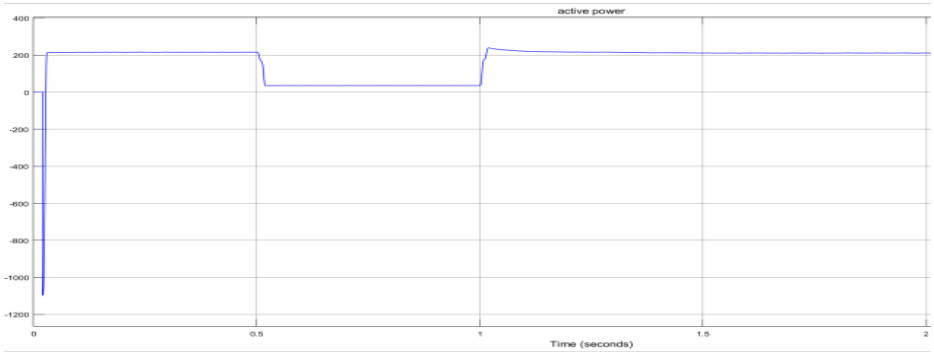

Fig.15. Active power for FLC MPPT

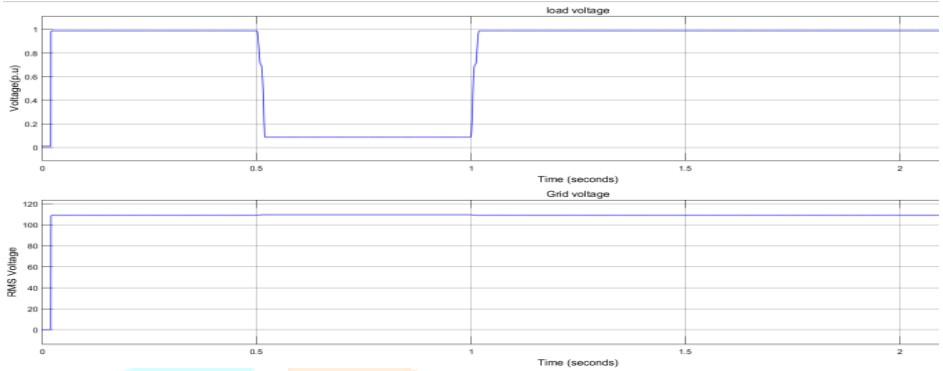

Fig.16. Load voltage and Grid voltages for ANN MPPT

Load voltage and grid voltage with ANN-MPPT is shown in fig.16. the RMS grid voltage is constant irrespective of load variations and load voltage is changing from 1 p.u to 0.1 p.u and then recovered to 1 p.u.

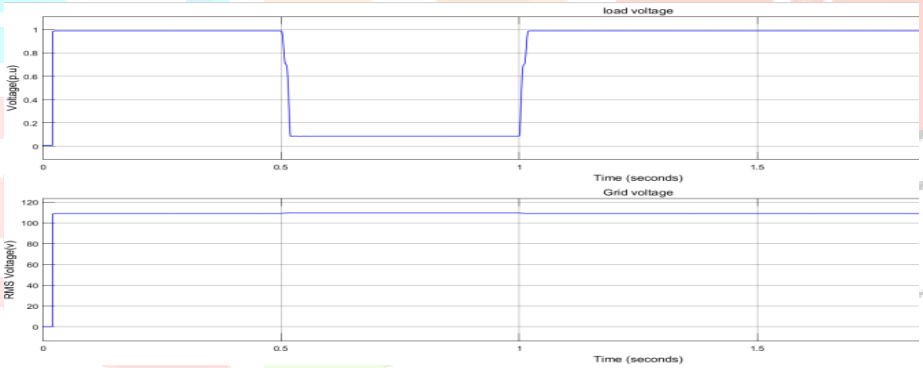

Fig.17. Load voltage and Grid voltages for FLC MPPT

Load voltage and grid voltage with FLC-MPPT is shown in fig.17. the RMS grid voltage is constant irrespective of load variations and load voltage is changing from 1 p.u to 0.1 p.u and then recovered to 1 p.u. Fig.10 to Fig.17 shows, Performance of proposed IDM in the worst case study which includes active power, load voltage and grid voltage. The presented outputs show that PCC voltage was successfully pushed to the lower bound and that exact Islanding detection was achieved in less than 700 milliseconds.

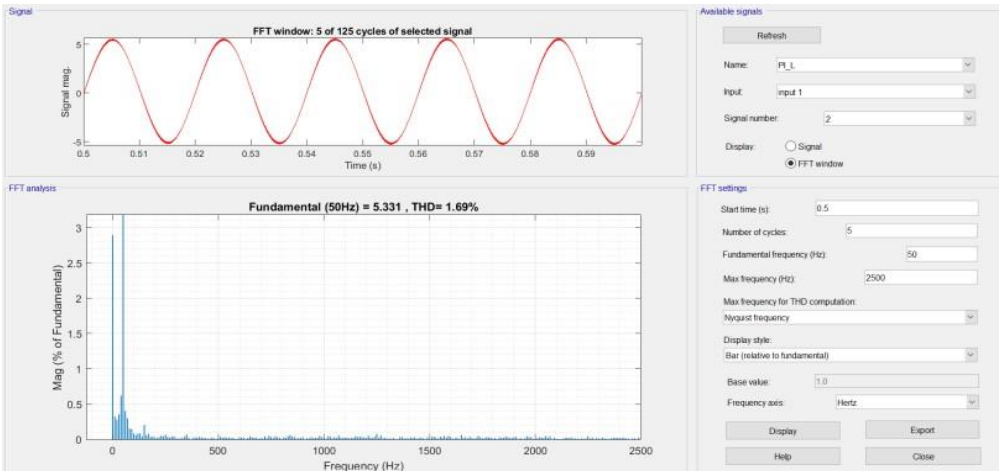

Fig.18. THDI for classic VPF

The isolated region's PCC voltage can be altered from its pre-Islanding setting (Vpr) to a new level after separation (Vpo) following Islanding. The magnitude of DG active power fluctuation, determines the post-Islanding voltage by triggering the embedded disturbance known as active power disturbance (P) [12]. While the relative active power mismatch/disturbance (P/PDG) is within the range [-29.13%, 17.35 %] for Vpr =1p.u., Vpo would be within the usual ranges, i.e. 0.88 to 1.10p.u., and Islanding would be undetectable by conventional voltage relays.

Harmonics in the electrical system cause voltage or current to deviate from their original sinusoidal wave patterns. THD, which is defined as the ratio of the root-mean-square (RMS) voltage or current of the harmonics to the fundamental component, may be used to measure this deviation. THDI should be kept below 5%, according to IEEE Standard 1547-2008 and IEC Standard 61727-2002. Initially, the study is carried out at various degrees of active power generation. Fig.18 to Fig.20 depicts the findings, which include THDI for classic VPF as well as new systems.

In addition, Fig.18 shows the harmonic spectra (for h < 20) in 25% of STC output power. THDI and the harmonic components, unlike VPF, are acceptable in the presence of the disturbance in the modified sliding-mode technique. THDI in VPF increases when the amplitude of the output current (power) decreases owing to a given disturbance magnitude. The disturbance magnitude of a sliding-mode IDM, on the other hand, is regulated in the voltage control loop (MPPT) using the DG's active power output. As a result, even in low-power production, it may deliver low THD. The suggested IDM's minimum output power level is 195 W, while the sample GCPVS's minimum output power level for traditional VPF with acceptable power quality is 285 W. This highlights the GCPVS's increased operating range and acceptable power quality when fitted with the proposed system.

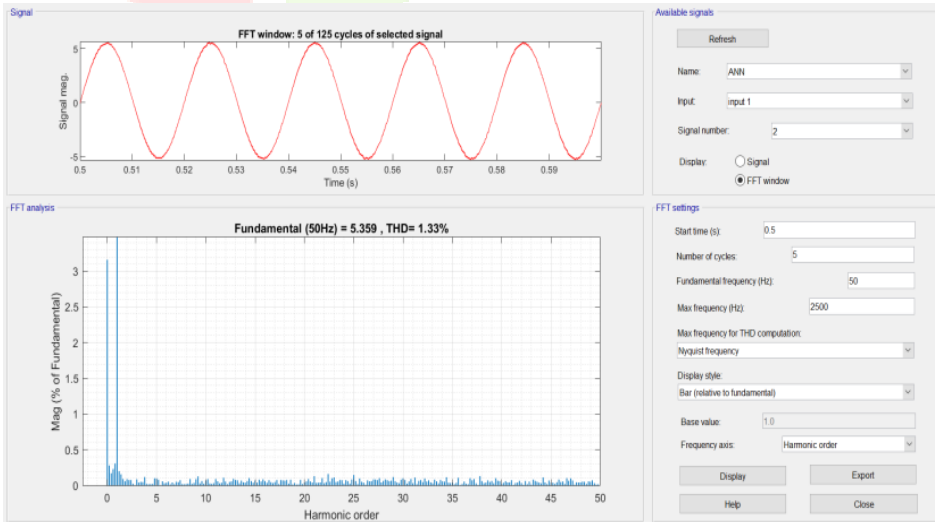

Fig.19. THDI for ANN MPPT

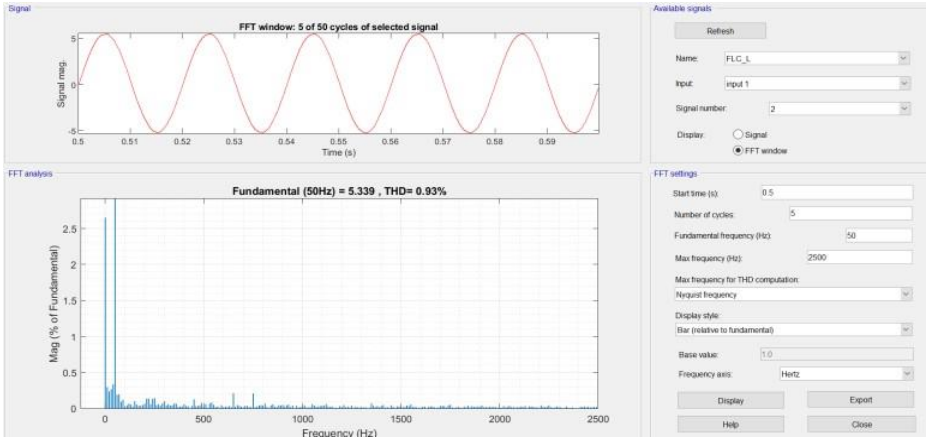

Fig.20. THDI for FLC MPPT

Table V : THD Comparison

S. NO	Method	THD (%)
1	VPF	1.69%
2	ANN-MPPT	1.33%
3	FLC-MPPT	0.93%

Table V shows THD comparison, from this table ANN-MPPT method reduces THD value by 21.30% as compared with VPF method. FCL-MPPT reduces THD by 44.97% and 30.07% as compared with VPF and ANN-MPPT methods.

Table VI : Settling Time Comparison

S.NO	Method	Settling Time(Sec)
1	VPF	1 sec
2	ANN-MPPT	0.5 sec
3	FLC-MPPT	0.1 sec

Form the Table VI The settling time of the FLC MPPT is 0.1 sec compared to the VPF method and ANN method, it reaches very short period, consequently the performance is increased.

VII. CONCLUSIONS

This paper proposes Fuzzy Logic Controller based Maximum Power Point Tracking method and Artificial Neural Network based Maximum Power Point Tracking methods. The proposed methods are designed and implemented in MATLAB/Simulink environment under different loading conditions. The results demonstrated that the ANN-MPPT is reducing the harmonics effectively as compared with VPF method. The FLC MPPT Settling time is very low compared to the conventional methods. The FLC-MPPT performance is better than the ANN-MPPT and VPF methods.

REFERENCES:

[1] A. Jäger-Waldau , “PV status report 2017,” Publications Office of theEuropean Union, Luxembourg, 2018.
[2] M. Sandhu and T. Thakur, “Harmonic minimization in a modified cascaded multilevel inverter for islanded microgrid using two switchingtechniques,” International Journal of Grid and Distributed Computing, vol. 10, no. 12, pp. 11-20, Dec. 2017.
[3] S. Natarajan and R. S. R. Babu, “Reduction of total harmonic distortion in cascaded H-bridge inverter by pattern search technique,” International Journal of Electrical and Computer Engineering (IJECE),vol. 7, no. 6, p. 3292, Dec. 2017.
[4] A. Luo, Q. Xu, F. Ma et al., “Overview of power quality analysis andcontrol technology for the smart grid,” Journal of Modern Power Systems and Clean Energy, vol. 4, no. 1, pp. 1-9, Jan. 2016.
[5] A. Khamis, H. Shareef, E. Bizkevelci et al., “A review of islanding detection techniques for renewable distributed generation systems,” Renewable and Sustainable Energy Reviews, vol. 28, pp. 483-493, Dec.2013.
[6] W. Xu, G. Zhang, C. Li et al., “A power line signaling based technique for anti-islanding protection of distributed generators part I:scheme and analysis,” IEEE Transactions on Power Delivery, vol. 22,no. 3, pp. 1758-1766, Jul. 2007.
[7] G. Bayrak, “A remote islanding detection and control strategy for photovoltaic-based distributed generation systems,” Energy Conversionand Management, vol. 96, pp. 228-241, May 2015.
[8] G. Bayrak and E. Kabalci, “Implementation of a new remote islandingdetection method for wind-solar hybrid power plants,” Renewable andSustainable Energy Reviews, vol. 58, pp. 1-15, May 2016.
[9] J. C. M. Vieira, D. S. Correa, W. Freitas et al., “Performance curvesof voltage relays for islanding detection of distributed generators,”IEEE Transactions on Power Systems, vol. 20, no. 3, pp. 1660-1662,Aug. 2005.

[10] J. C. M. Vieira, W. Freitas, W. Xu et al., "Performance of frequencyrelays for distributed generation protection," IEEE Transactions onPower Delivery, vol. 21, no. 3, pp. 1120-1127, Jul. 2006.
[11] Y. Shang, S. Shi, and X. Dong, "Islanding detection based on asymmetric tripping of feeder circuit breaker in ungrounded power distribution system," Journal of Modern Power Systems and Clean Energy,vol. 3, no. 4, pp. 526-532, Oct. 2015.
[12] E. Kamyab and J. Sadeh, "Islanding detection method for photovoltaicdistributed generation based on voltage drifting," IET Generation,Transmission& Distribution, vol. 7, no. 6, pp. 584-592, Jun. 2013.
[13] M. Bakhshi, R. Noroozian, and G. B. Gharehpetian, "Islanding detection scheme based on adaptive identifier signal estimation method,"ISA Transactions, vol. 71, pp. 328-340, Nov. 2017.
[14] M. Mishra, M. Sahani, and P. K. Rout, "An islanding detection algorithm for distributed generation based on Hilbert-Huang transform andextreme learning machine," Sustainable Energy, Grids and Networks,vol. 9, pp. 13-26, Mar. 2017.
[15] P. P. Das and S. Chattopadhyay, "A voltage-independent islanding detection method and low-voltage ride through of a two-stage PV inverter," IEEE Transactions on Industry Applications, vol. 54, no. 3, pp.2773-2783, May 2018.
[16] L. A. C. Lopes and H. Sun, "Performance assessment of active frequency drifting islanding detection methods," IEEE Transactions onEnergy Conversion, vol. 21, no. 1, pp. 171-180, Mar. 2006.
[17] A. Yafaoui, B. Wu, and S. Kouro, "Improved active frequency drift anti-islanding detection method for grid connected photovoltaic systems," IEEE Transactions on Power Electronics, vol. 27, no. 5, pp.2367-2375, May 2012.
[18] D. Reigosa, F. Briz, C. B. Charro et al., "Active islanding detectionusing high-frequency signal injection," IEEE Transactions on IndustryApplications, vol. 48, no. 5, pp. 1588-1597, Sep. 2012.
[19] T. Bei, "Accurate active islanding detection method for grid-tied inverters in distributed generation," IET Renewable Power Generation,vol. 11, no. 13, pp. 1633-1639, Nov. 2017.
[20] H. F. Xiao, Z. Fang, D. Xu et al., "Anti-islanding protection relay formedium voltage feeder with multiple distributed generators," IEEETransactions on Industrial Electronics, vol. 64, no. 10, pp. 7874-7885,Oct. 2017.
[21] P. Du, Z. Ye, E. E. Aponte et al., "Positive-feedback-based active ant islanding schemes for inverter-based distributed generators: basic principle, design guideline and performance analysis," IEEE Transactionson Power Electronics, vol. 25, no. 12, pp. 2941-2948, Dec. 2010.
[22] S. K. Kim, J. H. Jeon, H. K. Choi et al., "Voltage shift accelerationcontrol for anti-islanding of distributed generation inverters," IEEETransactions on Power Delivery, vol. 26, no. 4, pp. 2223-2234, Oct.2011.
[23] F. J. Lin, J. H. Chiu, Y. R. Chang et al., "Active islanding detectionmethod using d-axis disturbance signal injection with intelligent control," IET Generation, Transmission & Distribution, vol. 7, no. 5, pp.537-550, May 2013.
[24] A. Samui and S. R. Samantaray, "An active islanding detectionscheme for inverter-based DG with frequency dependent ZIP-exponential static load model," International Journal of Electrical Power & Energy Systems, vol. 78, pp. 41-50, Jun. 2016.
[25] R. Bakhshi and J. Sadeh, "Voltage positive feedback based activemethod for islanding detection of photovoltaic system with string inverter using sliding mode controller," Solar Energy, vol. 137, pp. 564577, Nov. 2016.
[26] IEEE Standard for Interconnecting Distributed Resources with ElectricPower Systems, IEEE Standard 1547-2008, 2008.
[27] Characteristics of the Utility Interface for Photovoltaic (PV) Systems,IEC 61727, 2002.
[28] G. A. Rampinelli, F. P. Gasparin, A. J. Bühler et al., "Assessment andmathematical modeling of energy quality parameters of grid connectedphotovoltaic inverters," Renewable and Sustainable Energy Reviews,vol. 52, pp. 133-141, Dec. 2015.
[29] M. Hamzeh and H. Mokhtari, "Power quality comparison of active islanding detection methods in a single phase PV grid connected inverter," In Proceedings of IEEE International Symposium on IndustrialElectronics (ISIE 2009), Seoul Olympic Parktel, Korea, Jul. 2009, pp.1-6.
[30] Y. Levron and D. Shmilovitz, "Maximum power point tracking employing sliding mode control," IEEE Transactions on Circuits and Systems I: Regular Papers, vol. 60, no. 3, pp. 724-732, Mar. 2013.
[31] IEEE Recommended Practice for Utility Interface of Photovoltaic (PV)Systems, IEEE Standard 929-2000, 2000.
[32] Q CELLS Official Website. (2018, Aug.). QPRO-G2 data. [Online].Available: www.q-cells.com.

Author's Profile:

Dr. P. SHASHAVALI Received his B.Tech Degree from JNT University Hyderabad. He Received Master of Technology Degree from G.Pulla Reddy Engineering College, Kurnool. Received Ph.D Degree from JNT University Anantapur. Presently he is working as Assistant Professor(C) in the Department of Electrical and Electronics Engineering ,S.K. University College of Engineering & Technology, S.K.University,Ananthapuramu-515003,Andhrapradesh,India.His research area of interest is Reliability concepts in power Electronic converters, Renewable Energy Sources and Facts Devices

Mr. C.A. BHASKAR has graduated his B.Tech from P.V.K.K Institute of Technology ,Ananthapuramu ,A.P. Currently he is pursuing M.Tech (Electrical Power Systems) from S. K. University College of Engineering and Technology, S.K. University ,Ananthapuramu-515003, A.P, India. His areas of interest are Electrical Machines and Power systems.